Collision of one-dimensional fermion clusters

Jun'ichi Ozaki, Masaki Tezuka, and Norio Kawakami
Department of Physics, Kyoto University, Kyoto JP-606-8502, Japan
(Received 17 April 2012; published 18 September 2012)

We study cluster-cluster collisions in one-dimensional Fermi systems with particular emphasis on the nontrivial quantum effects of the collision dynamics. We adopt the Fermi-Hubbard model and the time-dependent density-matrix renormalization-group method to simulate collision dynamics between two fermion clusters of different spin states with contact interaction. It is elucidated that the quantum effects become extremely strong with the interaction strength, leading to the transmittance being much more enhanced than expected from the semiclassical approximation. We propose a concise model as an application of the Bethe ansatz, which unveils the origin of the quantum effects and also explains the overall properties of the simulation results clearly. This model provides an intuitive perspective of the collision dynamics with contact interaction. Some potential applications, such as repeated collisions, are addressed.

DOI: 10.1103/PhysRevA.86.033621 PACS number(s): 03.75.Ss, 67.85.−d

I. INTRODUCTION

Recently, the nonequilibrium dynamics of cold atoms has attracted much attention because cold-atom systems are ideal as isolated quantum systems which can be experimentally designed [1]. In cold-atom systems, Feshbach resonance [2] has enabled experimentalists to modify the strength and sign of interactions between atoms. The dynamics of quantum quench [3–6] has been explored by suddenly changing the trap potential and the interaction, and also theoretically the quantum-quench dynamics has been studied [7–20].

Of these experiments, the dynamics of collision and mixing of two fermion clouds released from spin-dependent traps [21] motivates us to study collision dynamics between two fermion clusters in one-dimensional Fermi systems. For such one-dimensional collision dynamics, we have recently proposed a semiclassical model [22], so the fully quantum results and the semiclassical results can be theoretically compared. Thus, the differences between the two results, which we call the quantum effects, can be calculated. The one-dimensional collision dynamics [22–24] has been numerically studied from the interest in that experiment. It has been shown that the sign of the interaction does not affect the dynamics and that nontrivial quantum effects are dominant when the interaction is strong.

Analytically, the Bethe-ansatz exact solution [25–28] has successfully explained the properties of the static and homogeneous quantum systems with contact interaction in one dimension. In these integrable systems, the collision process can be expressed as a set of independent one-to-one collisions, so the wave functions are factorized. Thus, the physical quantities of the system can be analytically calculated with the quantum effects included. In particular, the Bethe ansatz has extensively been used for the exact treatment of the static or thermodynamic properties. Also, important progress has been made in the calculation of the correlation functions [25].

However, the Bethe ansatz cannot be straightforwardly applied to the dynamics in nonsteady or inhomogeneous systems although the essence of the collision processes is contained in the Bethe ansatz. A complete analysis in the collision dynamics in these systems is essential for an understanding of the quantum nonequilibrium dynamics since collision dynamics is one of the basic concepts of dynamics.

In this study we simulate the cluster-cluster collision dynamics in one-dimensional spin-1/2 Fermi systems with contact interaction and calculate the quantum many-body effects in the collision dynamics. Then we propose a quantum-collision model based on the idea of the Bethe ansatz, which contains only the one-to-one collision parameters. This model, which we call the independent-collision model (ICM), reproduces the simulation results well and fully elucidates the quantum effects of the collision dynamics, extremely enhancing the transmittance at strong interaction. The essence of the ICM is based on the Bethe ansatz idea, which can intuitively explain the collision dynamics with contact interaction although the ICM is an approximate description of the collision. We address two applications of the ICM, interaction-sign effects and repeated collisions.

II. SIMULATION

We conduct simulations of collision dynamics and calculate reflectance and transmittance of the clusters in one-dimensional spin-1/2 Fermi systems. Initially, n fermions per spin are trapped by spin-dependent potentials separately (Fig. 1) ($n \leqslant 6$ for numerically exact results). Both trap potentials are harmonic, and they have the same shape but are spatially separated. The mass of a fermion is m, the trap frequency of the harmonic potentials is ω (the oscillation cycle is $T = 2\pi/\omega$), and the interaction strength between the fermions is zero. So the typical width of the particle-density tails is $\eta = \sqrt{\hbar/m\omega}$. We set the distance between the centers of the initial potentials as $2D = 10\eta \gg \eta$ so that the overlap between the two clusters is negligible. The center of the spin-down (up) trap potential is $x = -D = -5\eta$ ($x = D = 5\eta$).

At $t = 0$, we suddenly change the trap potentials into a new shared potential, $V(x) = \frac{1}{2}m\omega^2x^2$. Simultaneously, we switch on the contact interaction between spin-up and spin-down fermions as $u\delta(x_d - x_u)$, where x_d (x_u) is the location of a spin-down (up) particle. Then the two clusters start moving towards each other without significantly changing their shapes, and they collide around $x = 0$ at $t = T/4$ with

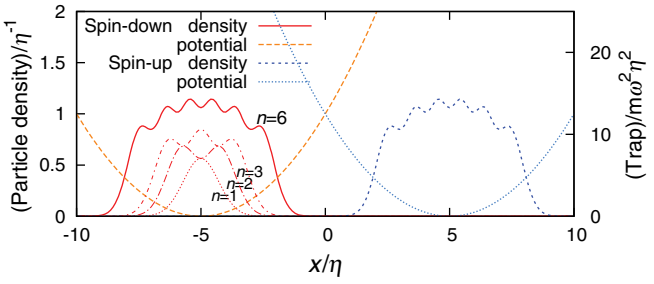

FIG. 1. (Color online) Initial particle density and trap potential at $n = 6$ and initial spin-down density at $n = 1$, $n = 2$, and $n = 3$.

an average momentum $|p| = m\omega D$. Finally, depending on the interaction strength u, they are reflected to the initial location or travel to the opposite location by $t = T/2$, and the particle density around $x = 0$ is almost zero again. So the number of reflected particles $N_n^{\mathrm{ref}}(u)$ and the number of transmitting particles $N_n^{\mathrm{tra}}(u)$ are obtained by counting the spin-down (up) particle number in $x < 0$ and $x > 0$ ($x > 0$ and $x < 0$). We obtain the reflectance $R_n(u) = N_n^{\mathrm{ref}}(u)/n$ and the transmittance $T_n(u) = N_n^{\mathrm{tra}}(u)/n$ [$R_n(u) + T_n(u) = 1$]. Clearly, $R_n(0) = 0, T_n(0) = 1$, and $R_n(\infty) = 1, T_n(\infty) = 0$ because the system is one dimensional.

We discretize the system to adopt the one-dimensional Fermi-Hubbard model and apply the time-dependent density-matrix renormalization-group (t-DMRG) method [29–31] to simulate the dynamics. We take 199 sites numbered $-99, -98, \ldots, +98, +99$ at regular intervals; the site -50 ($+50$) is the initial location of the potential center for spin-down (up) atoms. The lattice constant is $\delta x = 2D/100 = 0.1\eta$, which is small enough so that the umklapp scattering can be neglected. The value of the trap potential at site i is $V_{i,\sigma}(t) = \frac{1}{2}m\omega^2(x_i - \sigma D)^2$ ($\sigma = -$ for spin-down particles and $\sigma = +$ for spin-up). The discretized Hamiltonian is

$$\hat{H}(t) = -\frac{\hbar^2}{2m\delta x^2}\sum_{i,\sigma}(\hat{a}_{i,\sigma}^{\dagger}\hat{a}_{i+1,\sigma} + \hat{a}_{i+1,\sigma}^{\dagger}\hat{a}_{i,\sigma}) + \frac{u}{\delta x}\sum_i \hat{n}_{i,+}\hat{n}_{i,-} + \sum_{i,\sigma} V_{i,\sigma}(t)\hat{n}_{i,\sigma},$$

where $\hat{a}_{i,\sigma}$ annihilates an electron with spin σ on site i and $\hat{n}_{i,\sigma} \equiv \hat{a}_{i,\sigma}^{\dagger}\hat{a}_{i,\sigma}$. We calculate the time evolution by this Hamiltonian starting from the ground state of the system by the t-DMRG method up to $t = T/2$ in which the time step is $10^{-5}T$ and the maximum discarded eigenvalue of the reduced density matrix is $\varepsilon < 10^{-12}$. The simulation is conducted in the following range of parameters: the fermion number $n \leqslant 6$ and the contact-interaction strength $2^{-5} \leqslant u/u_c \leqslant 2^5$ ($u_c = 2\hbar p/m$).

Figure 2(a) shows the reflectance $R_n(u)$ obtained by the DMRG simulation for $2^{-5} \leqslant u/u_c \leqslant 1$. The figure implies $R_n(u) \propto u^2$ in the small-u limit. We also plot the ratio $R_n(u)/R_1(u)$ in Fig. 2(b) to evaluate the many-body effects. It is observed that $R_n(u) \simeq nR_1(u)$ is approached in the limit of $u \to 0$. In this limit, almost all particles transmit, and a particle collides with the n particles of different spin before it reaches the opposite side. So in the semiclassical picture,

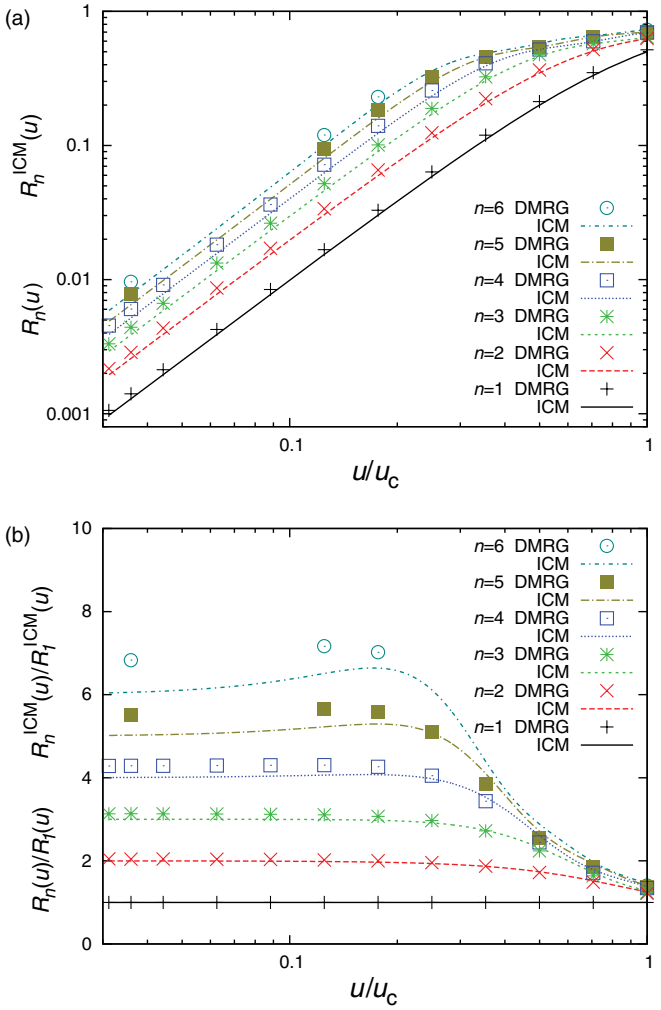

FIG. 2. (Color online) (a) Reflectance obtained by DMRG simulation $R_n(u)$ (dots) and that by ICM $R_n^{\mathrm{ICM}}(u)$ (lines) (log scale on x and y axes). (b) Reflectance ratio obtained by DMRG simulation $R_n(u)/R_1(u)$ (dots) and that by ICM $R_n^{\mathrm{ICM}}(u)/R_1^{\mathrm{ICM}}(u)$ (lines) (log scale on x axis).

the reflectance is $nR_1(u)$ because the number of the reflected particles is approximately $n^2R_1(u)$. Therefore, there is no quantum effect in this limit [22]. On the other hand, Fig. 3(a) shows the transmittance $T_n(u)$ from the DMRG simulation for $1 \leqslant u/u_c \leqslant 2^5$. The figure shows $T_n(u) \propto u^{-2}$ in the large-u limit. We plot the ratio $T_n(u)/T_1(u)$ in Fig. 3(b), which illustrates $T_n(u) \simeq nT_1(u)$ as $u \to \infty$. In this limit, since almost all particles are reflected, in most cases a particle collides with another particle of different spin just once during a cluster-cluster collision. So in the semiclassical case, the number of the transmitting particles is almost $nT_1(u)$, so the transmittance is $T_1(u)$. Therefore, there are strong quantum effects in this limit [22], and the transmittance in the quantum case is n times larger than in the semiclassical case. These quantum effects are calculated by the difference between the semiclassical and quantum-simulation results, but their origin has not been understood. However, in this study a sufficient explanation of these quantum effects is given by a concise model below.

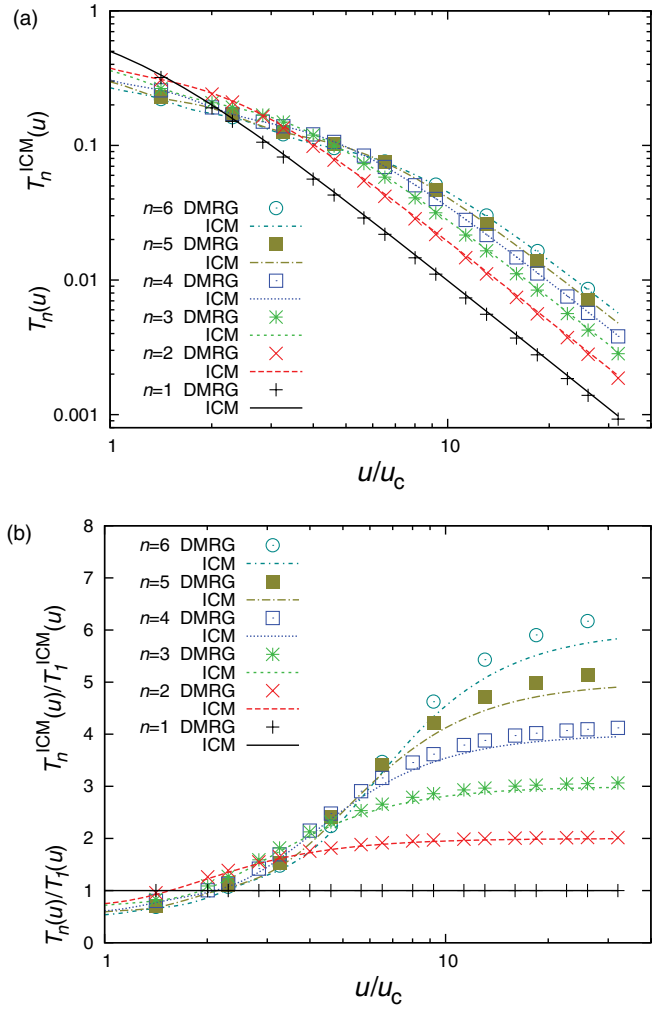

FIG. 3. (Color online) (a) Transmittance obtained by DMRG simulation $T_n(u)$ (dots) and that by ICM $T_n^{\rm ICM}(u)$ (lines) (log scale on x and y axes). (b) Transmittance ratio obtained by DMRG simulation $T_n(u)/T_1(u)$ (dots) and that by ICM $T_n^{\rm ICM}(u)/T_1^{\rm ICM}(u)$ (lines) (log scale on x axis).

III. MODEL

We propose the independent-collision model to explain the simulation results. This model is regarded as an application of the Bethe ansatz [25–28] to inhomogeneous systems as will be discussed later.

We start from the simplest case, the one-to-one collision dynamics, which can be easily calculated. The initial wave function is $|\downarrow\uparrow\rangle$, meaning that a spin-down (up) particle is on the left (right). When the spin-down-particle wave packet with momentum p and the spin-up-particle wave packet with momentum $-p$ collide, $|\downarrow\uparrow\rangle$ splits into $\rho\,|\downarrow\uparrow\rangle$ (reflection term) and $\tau\,|\uparrow\downarrow\rangle$ (transmission term), and the momenta are reversed, where we approximately have $\rho = u/(iu_c - u)$ and $\tau = iu_c/(iu_c - u)$. The theoretical reflectance $R_1^{\rm ICM}(u)$ and transmittance $T_1^{\rm ICM}(u)$ are approximately calculated by the coefficients of $|\downarrow\uparrow\rangle$ and $|\uparrow\downarrow\rangle$ as

$$R_1^{\rm ICM}(u) = |\rho|^2 = \frac{u^2}{u_c^2 + u^2}, \quad T_1^{\rm ICM}(u) = |\tau|^2 = \frac{u_c^2}{u_c^2 + u^2}.$$

Next, we regard the multiparticle cases as a series of one-to-one collisions. In this system, the initial wave function can be expressed as a Slater determinant for spin-polarized particles. We set up the single-particle wave functions of spin-down particles as $\varphi_{-1}(x), \varphi_{-2}(x), \ldots, \varphi_{-n}(x)$ and those of spin-up particles as $\varphi_1(x), \varphi_2(x), \ldots, \varphi_n(x)$. So the initial wave function of the whole system is $\psi = (n!)^{-1}|\varphi_{-i}(x_{-j})|_\downarrow|\varphi_i(x_j)|_\uparrow$, where the variables in the determinant $|\cdot|_\downarrow(|\cdot|_\uparrow)$ belong to spin-down (up) particles. We can take these single-particle wave functions not only as the eigenstates of the initial Hamiltonian but also as the localized wave functions created by a unitary basis transformation. It is convenient to use the localized single-particle wave functions to analyze the cluster-cluster collision. Because of the contact interaction, there is no difference in the shapes of the single-particle wave function before and after a one-to-one collision. However, the whole wave function splits into the unchanged part (transmission term) and a spin-flipped part (reflection term) after a one-to-one collision. Therefore, if the n^2 one-to-one collisions occur independently, the time evolution of the system is described by (i) the time evolution of the single-particle wave functions and (ii) the splits of the wave functions at the one-to-one collisions. The time evolution (i) occurs in each $\varphi_{\pm i}(x)$, and the form of $\varphi_{\pm i}(x)$ is changed, but this evolution does not change the expression of $\psi = (n!)^{-1}|\varphi_{-i}(x_{-j})|_\downarrow|\varphi_i(x_j)|_\uparrow$. On the other hand, at the time evolution (ii), the wave function splits into the transmission term and the reflection term. When the particle a and the particle b collide, ψ splits into $\tau\psi + \rho F_b^a\psi$ (F_b^a is the flip operator of φ_a and φ_b). Even when a and b have the same spin, this relation is applicable because $\tau + \rho F_b^a = 1$ for the particles of the same spin.

We assume that $\varphi_i(x)$ is localized at x_i ($x_{-n} < \cdots < x_{-1}$ and $x_1 < \cdots < x_n$), that the time evolution (i) is expressed as the motion of x_i, and that φ_i independently collides only with the wave functions of the reversed momentum localized at the same location. This assumption of the independent-ordered collision, which corresponds to the factorizability of the Bethe ansatz [25–28], is supported also numerically later. Since the movement of x_i is similar to the case of classical dynamics, the ordering of the collisions is the same (see Fig. 4, which is discussed below). The initial wave function of the whole system is expressed as $\psi = |\downarrow^{-n}\cdots\downarrow^{-1}\uparrow^1\cdots\uparrow^n\rangle$, meaning that there are spin-down particles at x_i ($i < 0$) and spin-up particles at x_j ($j > 0$) and that the ordering of the wave function in the Slater determinant is adjusted to the

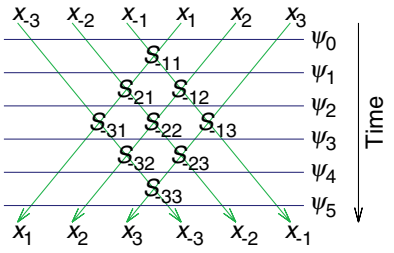

FIG. 4. (Color online) Collision order in ICM at $n = 3$. S_{-ij} is the one-to-one collision between φ_{-i} and φ_j, and ψ_k is the wave function after the kth set of collisions. Simultaneous collisions are commutative.

one-dimensional ordering of x_i. The first one-to-one collision occurs between x_{-1} and x_1. So the wave function splits into

$$\tau_{-11}\,|\cdots\downarrow^{-2}\downarrow^{-1}\uparrow^{1}\uparrow^{2}\cdots\rangle+\rho_{-11}\,|\cdots\downarrow^{-2}\uparrow^{-1}\downarrow^{1}\uparrow^{2}\cdots\rangle\,,$$

but the order of x_{-1} and x_1 is reversed, so the expression

$$\rho_{-11}\,|\cdots\downarrow^{-2}\downarrow^{1}\uparrow^{-1}\uparrow^{2}\cdots\rangle+\tau_{-11}\,|\cdots\downarrow^{-2}\uparrow^{1}\downarrow^{-1}\uparrow^{2}\cdots\rangle$$

corresponds to the spatial-spin distribution in which ρ_{-11} and τ_{-11} are the collision parameters between the two wave packets of x_{-1} and x_1. Simultaneous collisions are commutative, so we can assume that one of them occurs earlier. The next collision is assumed to be between x_{-2} and x_1 (simultaneously x_{-1} and x_2), and then $|\cdots\downarrow^{-2}\downarrow^{1}\uparrow^{-1}\uparrow^{2}\cdots\rangle$ is not changed, but for the sign of the Slater determinant, the spatial-spin distribution expression is

$$|\cdots\downarrow^{-2}\downarrow^{1}\uparrow^{-1}\uparrow^{2}\cdots\rangle=-\,|\cdots\downarrow^{1}\downarrow^{-2}\uparrow^{-1}\uparrow^{2}\cdots\rangle\,.$$

By omitting the ordering of x_i from this expression, we obtain a simplified expression of the system wave function. It is possible to calculate the outcome of the cluster-cluster collision by calculating the system wave function after n^2 one-to-one collisions between all possible combinations of x_i $(i<0)$ and x_j $(j>0)$ because the single-particle wave functions evolve as those of free particles and they collide n times during the half-cycle of the oscillation.

Using the simplified expression, the cluster-cluster collision is calculated in the following process. The initial wave function is simplified as $|\downarrow\cdots\downarrow\uparrow\cdots\uparrow\rangle$ with n $\downarrow$'s and n $\uparrow$'s. The cluster-cluster collision is described by a series of one-to-one collisions. For a collision between $\downarrow$ and $\uparrow$, the wave function splits into a reflection term (amplitude ρ_{ij}) and a transmission term (amplitude τ_{ij}). For a collision between two particles of the same spin, the wave function is multiplied by -1. The ordering of the one-to-one collisions is the same as in classical dynamics, shown in Fig. 4. The first collision occurs at the center of the system, and the second collisions occur at the locations next to the center $(n\geqslant 2)$. The third collisions arise at the center and at the two locations away from the center $(n\geqslant 3)$. Finally, all the particles have reversed momenta, and then collision dynamics finishes. The external parameters of the ICM are only ρ_{ij} and τ_{ij}, which are of the one-to-one collision. Since the calculations for large n are complicated, we numerically compute the ICM reflectance $R_n^{\mathrm{ICM}}(u)$ and the ICM transmittance $T_n^{\mathrm{ICM}}(u)$, where approximately ρ_{ij} and τ_{ij} are set as constants (ρ and τ).

The ICM focuses on the dynamics of the localized single-particle wave packets, namely, if the centers of the wave functions of the same spin are separated from each other by a distance on the order of their typical width, the effect of the interaction at the time of the collision between the centers of the wave functions of different spins is independent of the effects of collisions occurring at other parts of the system.

This idea is analytically supported by the Bethe ansatz [25–28]. In the static case, the one-dimensional collision process of clusters can be divided into the independent one-to-one collisions. In fact, the two-body contact interaction makes the derivative of the many-body wave function discontinuous at the point where two particles coincide. In the static Bethe-ansatz solution, the effect of the contact interaction for each pair of up-spin and down-spin is independent of each other so that the wave function is factorized [25–28]; the one-to-one collisions can be calculated independently. The ICM is equivalent to the approximate factorizability in the dynamics of the wave packets.

IV. DISCUSSION

We plot the reflectance obtained by the ICM $R_n^{\mathrm{ICM}}(u)$ in Fig. 2(a) and the ratio $R_n^{\mathrm{ICM}}(u)/R_1^{\mathrm{ICM}}(u)$ in Fig. 2(b) for $u/u_c\leqslant 1$. The figure exhibits that $R_n^{\mathrm{ICM}}(u)$ agrees fairly well with $R_n(u)$ (the DMRG simulation loses accuracy in the limit of $u\to 0$), and the ICM is valid in the region. We discuss the asymptotic behavior of $R_n^{\mathrm{ICM}}(u)$ as $u\to 0$. In this limit, the dominant terms of $R_n^{\mathrm{ICM}}(u)$ are the coefficients of the single-reflection wave functions (wave functions after only one reflection) since almost all particles transmit in this limit. The coefficients of the single-reflection wave functions are $\rho\tau^{n-1}$, and the number of the single-reflection wave functions is n^2, so $R_n^{\mathrm{ICM}}(u)\simeq n^2|\rho\tau^{n-1}|^2/n\simeq n(u/u_c)^2$ is the asymptotic form. This analytical calculation is free from the interference effects, so the absence of quantum effects in the limit of $u\to 0$ is supported by the ICM. Figure 3 also shows the ICM result $T_n^{\mathrm{ICM}}(u)$ [Fig. 3(a)] and the ratio $T_n^{\mathrm{ICM}}(u)/T_1^{\mathrm{ICM}}(u)$ [Fig. 3(b)] for $1\leqslant u/u_c$. The figure shows that $T_n^{\mathrm{ICM}}(u)$ is consistent with $T_n(u)$ (the difference comes from the quantum fluctuation of the collision location and the collision momentum), so the ICM is correct in the region too. The asymptotic behavior of $T_n^{\mathrm{ICM}}(u)$ in the limit of $u\to\infty$ is dominated by the coefficient of the component with a single transmission, $|\downarrow\cdots\downarrow\uparrow\downarrow\uparrow\cdots\uparrow\rangle$. The coefficient is $\rho^{n-1}\tau(1+\rho^2+\cdots+\rho^{2n-2})$, so in the limit of $u\to\infty$ for fixed n, $T_n^{\mathrm{ICM}}(u)\simeq|\rho^{n-1}\tau(1+\rho^2+\cdots+\rho^{2n-2})|^2/n\simeq n(u/u_c)^{-2}$ is the asymptotic form. Differently from the small-u case, this term contains the interference effect. In the semiclassical picture in which all the horizontally aligned segments of the particle trajectories in Fig. 4 are independently spin down or spin up at some probability determined by the previous stage, the interference vanishes, and the transmittance becomes $|\rho^{n-1}\tau|^2(1^2+|\rho^2|^2+\cdots+|\rho^{2n-2}|^2)/n\simeq(u/u_c)^{-2}$. Therefore, the quantum transmittance is n times larger than the classical transmittance. Thus, the ICM explains the quantum effects in the large-u limit.

The ICM is consistent with the DMRG simulation, but we have assumed the independent-ordered collision to derive the ICM. To support this assumption numerically, we have also studied the following system. Initially, n fermions per spin are trapped separately, and the parameters of the particles are the same as those in the DMRG simulation of a cluster-cluster collision (Fig. 5). However, the trap potentials of both spins are not harmonic, but the combination of two harmonic potentials and the distance between these harmonic potentials is d. The harmonic centers of the spin-down (up) particles are at $x=-D,-D-d$ $(x=+D,+D+d)$ $(D=5\eta)$.

At $t=0$, we suddenly give a momentum p to the spin-down particles and a momentum $-p$ to the spin-up particles $(p=m\omega D)$, and simultaneously, we switch off the trap potentials and set the contact interaction between spin-up and spin-down fermions as $u\delta(x_1-x_2)$. The two clusters start moving at the velocity $|v|=p/m$, and they collide at $x=0$;

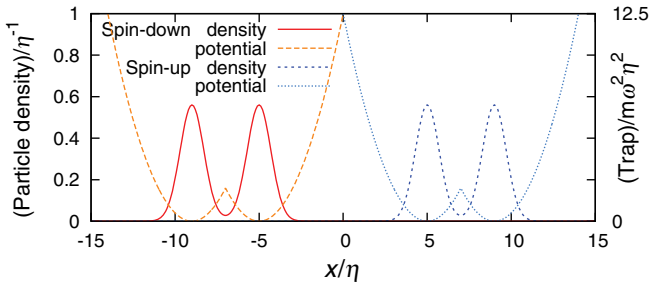

FIG. 5. (Color online) Initial particle density and trap potential at $n = 2$ and $d = 4\eta$.

then we calculate the reflectance $R_n^{\rm dist}(u,d)$. Except for the difference in the distribution of the momentum or the decay of the wave function, $R_n^{\rm dist}(u,0)$ should reproduce $R_n(u)$. To simulate the system, we use the same method under the same condition as in the DMRG simulation above, excepting the following conditions. We calculate the time evolution up to $t = (2D + d)/(v - 2\sqrt{m\omega\hbar}/m)$ for $n = 2$, $u/u_c = 0.5, 1.0, 2.0$, and $0 \leqslant d \leqslant 4\eta$ ($\sqrt{m\omega\hbar}$ is the initial momentum variation). We take 299 sites numbered $-149, -148, \ldots, +148, +149$ at regular intervals, but the lattice constant $\delta x = 0.1\eta$ is the same. The result of the simulation is that $|R_n^{\rm dist}(u,d) - R_n^{\rm dist}(u,0)|$ is under 1.5% for all u, so we conclude that the initial particle distribution has little effect on collision dynamics. Thus, if we calculate the cluster-cluster collision, we can simplify the system by assuming that initially the fermions are independently localized and independently collide. In the simplified dynamics, the wave function of the system splits after every independent collision, and the ordering of the independent collisions is the same as in classical dynamics. Therefore, the assumption of the independent-ordered collision is numerically supported.

As an application of the ICM, we discuss the effects of the interaction sign in the cluster-cluster collision. In one-dimensional collision dynamics, the sign of the contact interaction u does not affect the dynamics [22,23], and this property can be explained by the ICM. The imaginary unit i is contained only in ρ and τ in the ICM. Since physical quantities such as particle density are real, the values of these quantities are not changed if we substitute $-i$ for i. After the substitution, $\rho(u)$ and $\tau(u)$ become $\rho(-u)$ and $\tau(-u)$. This proves that the physical quantities do not depend on the sign of the interaction.

Another application of the ICM is the repeated cluster-cluster collision under the harmonic potential in which the kth collision occurs at $(k-1)T/2 < t < kT/2$. The dynamics of the multiple cluster-cluster collisions has been simulated by Peotta *et al.* [24]; the motion of the center of mass is a linear function of t in a region of strong interaction. We simulate this multiple cluster-cluster collision by the ICM and calculate the wave function after the kth collision by using the final state after the $(k-1)$th collision as the initial state. We use their system parameters [24] and assume the location of the localized wave functions $x_{-i} = -D - [i - (N+1)/2]\eta$ and $x_i = D + [i - (N+1)/2]\eta$ $(i > 0)$. Thus, we obtain results that agree very well with their Fig. 3(b). Therefore, the ICM is also useful for simulating the dynamics of the multiple cluster-cluster collisions.

V. CONCLUSION

In summary, using the time-dependent density-matrix renormalization-group method and the Fermi-Hubbard model, we have calculated the collision dynamics between two fermion clusters with contact interaction. We have introduced the independent-collision model for cluster-cluster collisions, which is based on the essence of the Bethe ansatz. We have also numerically checked the validity of the model by showing that the initial distribution of particles does not affect the collision dynamics. The independent-collision model has reproduced the simulation results and explained the large enhancement in the transmittance at strong interaction. Furthermore, we have demonstrated its potential applications to the interaction-sign effect and the repeated collision dynamics.

ACKNOWLEDGMENTS

This work was partially supported by a Grant-in-Aid for the Global COE Program "The Next Generation of Physics, Spun from Universality and Emergence" from MEXT of Japan. N.K. is supported by KAKENHI (Grants No. 21740232 and No. 20104010) and JSPS through its FIRST Program. J.O. is supported by a JSPS Research Fellowship for Young Scientists.

[1] D. Jaksch and P. Zoller, Ann. Phys. (Amsterdam, Neth.) **315**, 52 (2005).
[2] C. Chin, R. Grimm, P. Julienne, and E. Tiesinga, Rev. Mod. Phys. **82**, 1225 (2010).
[3] T. Kinoshita, T. Wenger, and D. S. Weiss, Nature (London) **440**, 900 (2006).
[4] L. E. Sadler, J. M. Higbie, S. R. Leslie, M. Vengalattore, and D. M. Stamper-Kurn, Nature (London) **443**, 312 (2006).
[5] S. Riedl, E. R. S. Guajardo, C. Kohstall, J. H. Denschlag, and R. Grimm, New J. Phys. **13**, 035003 (2011).
[6] U. Schneider, L. Hackermüller, J. P. Ronzheimer, S. Will, S. Braun, T. Best, I. Bloch, E. Demler, S. Mandt, D. Rasch, and A. Rosch, Nat. Phys. **8**, 213 (2012).
[7] K. Braun-Munzinger, J. A. Dunningham, and K. Burnett, Phys. Rev. A **69**, 053613 (2004).
[8] K. Sengupta, S. Powell, and S. Sachdev, Phys. Rev. A **69**, 053616 (2004).
[9] P. Calabrese and J. Cardy, Phys. Rev. Lett. **96**, 136801 (2006).
[10] M. Rigol, A. Muramatsu, and M. Olshanii, Phys. Rev. A **74**, 053616 (2006).
[11] A. Das, K. Sengupta, D. Sen, and B. K. Chakrabarti, Phys. Rev. B **74**, 144423 (2006).
[12] C. Kollath, A. M. Lauchli, and E. Altman, Phys. Rev. Lett. **98**, 180601 (2007).
[13] S. R. Manmana, S. Wessel, R. M. Noack, and A. Muramatsu, Phys. Rev. Lett. **98**, 210405 (2007).

[14] V. Gritsev, E. Demler, M. Lukin, and A. Polkovnikov, Phys. Rev. Lett. **99**, 200404 (2007).
[15] I. Klich, C. Lannert, and G. Refael, Phys. Rev. Lett. **99**, 205303 (2007).
[16] D. Rossini, A. Silva, G. Mussardo, and G. E. Santoro, Phys. Rev. Lett. **102**, 127204 (2009).
[17] P. Barmettler, M. Punk, V. Gritsev, E. Demler, and E. Altman, Phys. Rev. Lett. **102**, 130603 (2009).
[18] M. Rigol, Phys. Rev. Lett. **103**, 100403 (2009).
[19] A. Iucci and M. A. Cazalilla, Phys. Rev. A **80**, 063619 (2009).
[20] S. R. Manmana, S. Wessel, R. M. Noack, and A. Muramatsu, Phys. Rev. B **79**, 155104 (2009).
[21] A. Sommer, M. Ku, G. Roati, and M. W. Zwierlein, Nature (London) **472**, 201 (2011).
[22] J. Ozaki, M. Tezuka, and N. Kawakami, arXiv:1107.0774.
[23] J. Kajala, F. Massel, and P. Törmä, Eur. Phys. J. D **65**, 91 (2011).
[24] S. Peotta, D. Rossini, P. Silvi, G. Vignale, R. Fazio, and M. Polini, Phys. Rev. Lett. **108**, 245302 (2012).
[25] F. H. L. Essler, H. Frahm, F. Gohmann, A. Klumper, and V. E. Korepin, *The One-Dimensional Hubbard Model* (Cambridge University Press, Cambridge, 2005).
[26] J. B. McGuire, J. Math. Phys. (Melville, NY, US) **6**, 432 (1965).
[27] C. N. Yang, Phys. Rev. Lett. **19**, 1312 (1967).
[28] H. Bethe, Z. Phys. **71**, 205 (1931).
[29] S. R. White and A. E. Feiguin, Phys. Rev. Lett. **93**, 076401 (2004).
[30] U. Schollwöck, Rev. Mod. Phys. **77**, 259 (2005).
[31] K. A. Hallberg, Adv. Phys. **55**, 477 (2006).